

Figure 6-13 H<sub>2</sub> permeance as a function of time for membrane C01-F08 at 500, 550 and 600°C

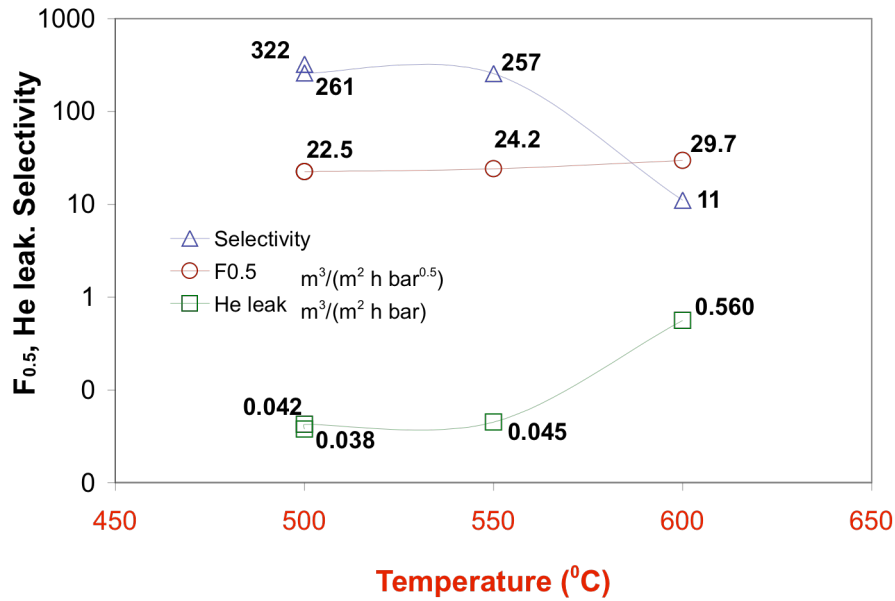


Figure 6-14 Selectivity (H<sub>2</sub>/He), H<sub>2</sub> permeance and He leak for membrane C01-F08 at 500, 550 and 600°C

At the end of the H<sub>2</sub> characterization the selectivity of the membrane was only 11. Pinholes were estimated to be as large as 1.6 μm in diameter from the He permeance vs. P<sub>ave</sub> data (see Section 10.3.1.1).

Membranes prepared on graded PH supports showed very good H<sub>2</sub> permeance stability. That is, no decline in H<sub>2</sub> permeance was observed at 500°C for over 1000 hr (Ma-32b). The reasons for such an outstanding stability of Pd composite membranes on PH were due to the type of oxide that is formed on PH supports. The oxide structure formed on PSS and PH supports and their effect on long term H<sub>2</sub> permeance stability is studied with great detail in Chapter 8. In addition, the presence of the Al<sub>2</sub>O<sub>3</sub> grade layer significantly reduced intermetallic diffusion in C01-F08 membrane. Therefore, the long term H<sub>2</sub> permeance stability of Ma-32b/34b/42 was also due to the presence of the Al<sub>2</sub>O<sub>3</sub> grade layer.

#### 6.3.3.2 *The grade layer as intermetallic diffusion barrier*

The following section aimed at the understanding of the ability of the Al<sub>2</sub>O<sub>3</sub> grade layer to mitigate intermetallic diffusion. After the H<sub>2</sub> characterization at 250°C, the porous section of membrane C01-F09 was cut in three pieces and each piece was heat-treated at a different temperature in order to investigate the temperature stability of the grade layer. It was especially desired to establish if the grade layer could reduce or inhibit the diffusion of Fe, Cr and Ni from the PSS support into the Pd dense film at 500°C. The temperature treatment of samples cut out of C01-F09 membranes was performed in H<sub>2</sub> atmosphere at 400, 500 and 600°C for 48 hr.

Figure 6-15(a), (b) and (c) represent the cross-section of three different samples from C01-F09 heated at 400, 500 and 600°C respectively. The structure and morphology of the grade layer in Figure 6-15(a) and (b) are the same as the grade layer seen in Figure 6-2. Therefore, no visible structural changes occurred at temperatures equal to or higher than 500°C. However, at 600°C, intermetallic diffusion led to the white patches seen in the grade layer as well as white patches seen on the stainless steel particles (diffusion of Pd into the stainless steel particles and vice versa).

Figure 6-16 and Figure 6-17 show the elemental composition across the grade layer for the sample heated at 500°C and 600°C respectively. Both elemental composition lines were performed at a position where the grade layer was around 5µm thick. The traces of Fe, Cr and Ni fell below the detection limit within the first micron of the grade layer in the sample heated at 500°C (Figure 6-16). Therefore, the grade layer successfully protected the selective Pd layer from intermetallic diffusion at 500°C. The Fe, Cr and Ni traces were visible all across the grade layer for the sample heated at 600°C indicating that intermetallic diffusion occurred through the fine grain structure of the grade layer at 600°C. However, no traces of Fe, Cr and Ni were detected in the dense Pd layer.

The Al<sub>2</sub>O<sub>3</sub> grade layer was very porous since only 15-25% of the porous support's initial He permeance was lost after its deposition in the case of C01-F09 and Ma-42 membranes. Therefore, even if intermetallic diffusion occurred in the Al<sub>2</sub>O<sub>3</sub> grade layer no H<sub>2</sub> permeance decline should be observed since H<sub>2</sub> mostly diffused as molecular H<sub>2</sub> through the porosity of the Al<sub>2</sub>O<sub>3</sub> grade layer. In summary, the grade layer effectively protected the dense Pd film from intermetallic diffusion at temperatures equal to or lower than 500°C.

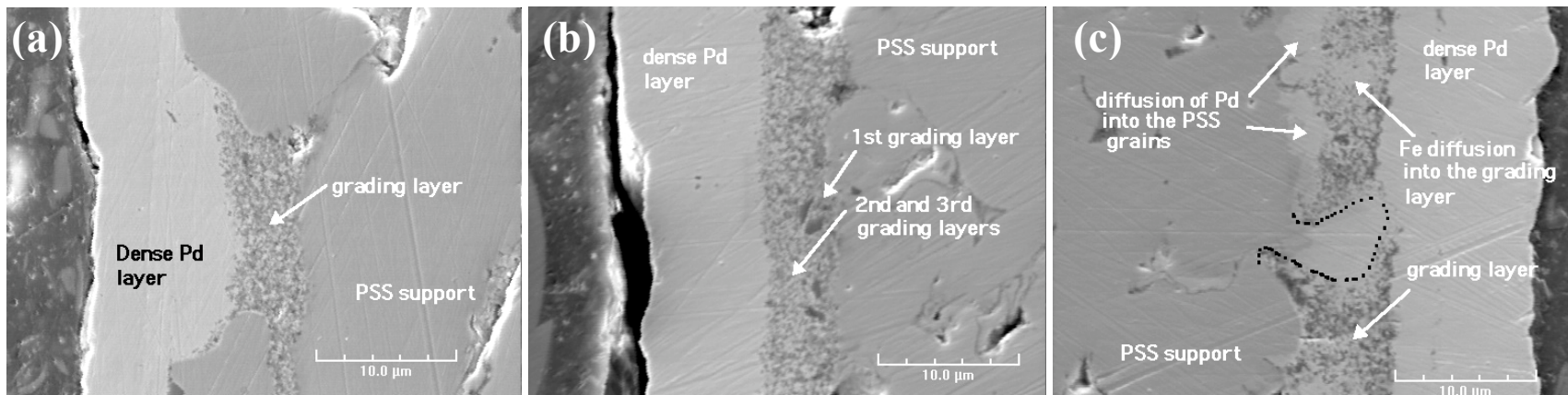


Figure 6-15 Sections of C01-F09 heated at (a) 400°C, (b) 500°C and (c) 600°C. Mag:2000X

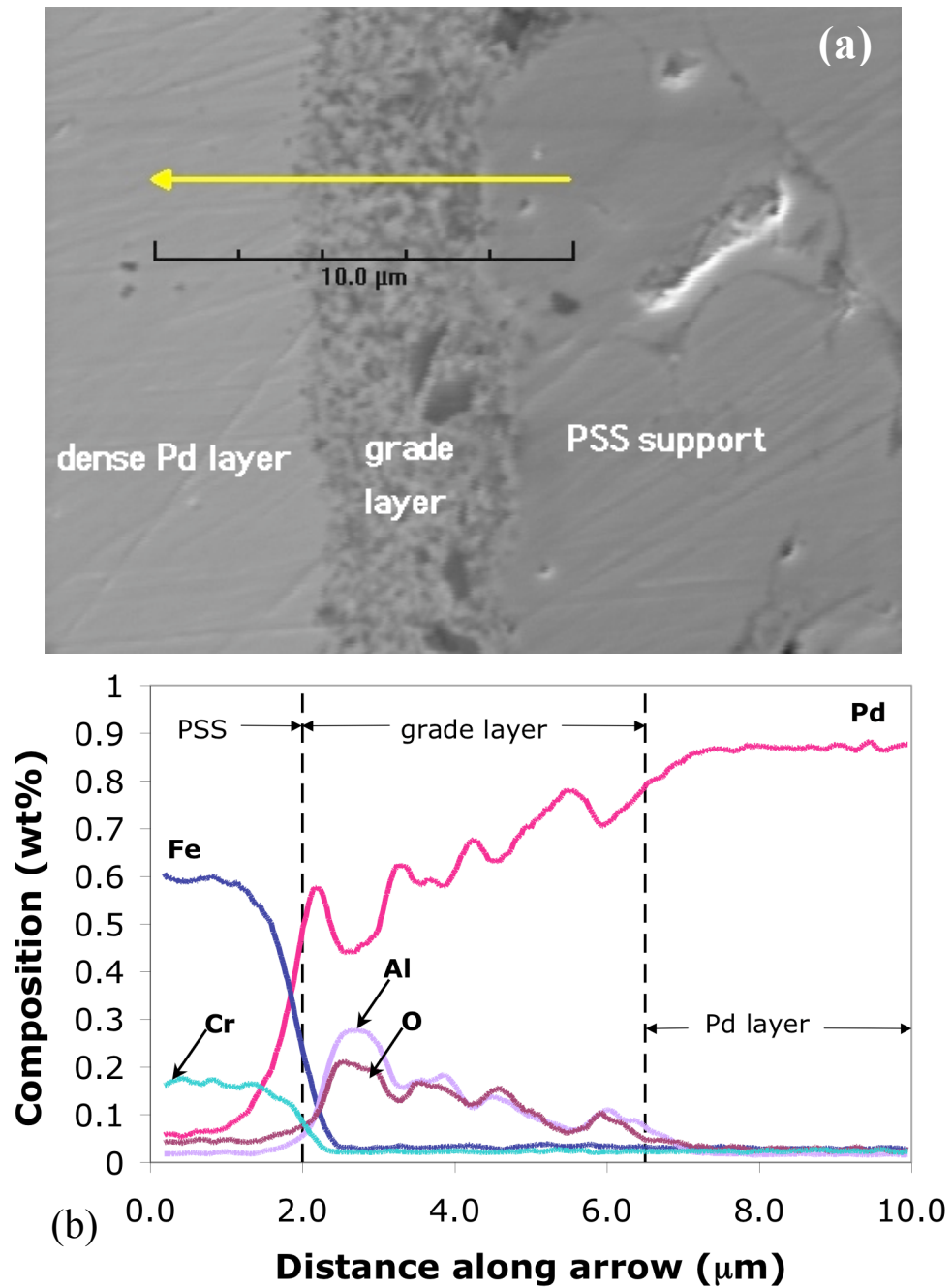


Figure 6-16 Composition analysis across the grade layer for the sample heated at  $500^\circ\text{C}$  in  $\text{H}_2$ .

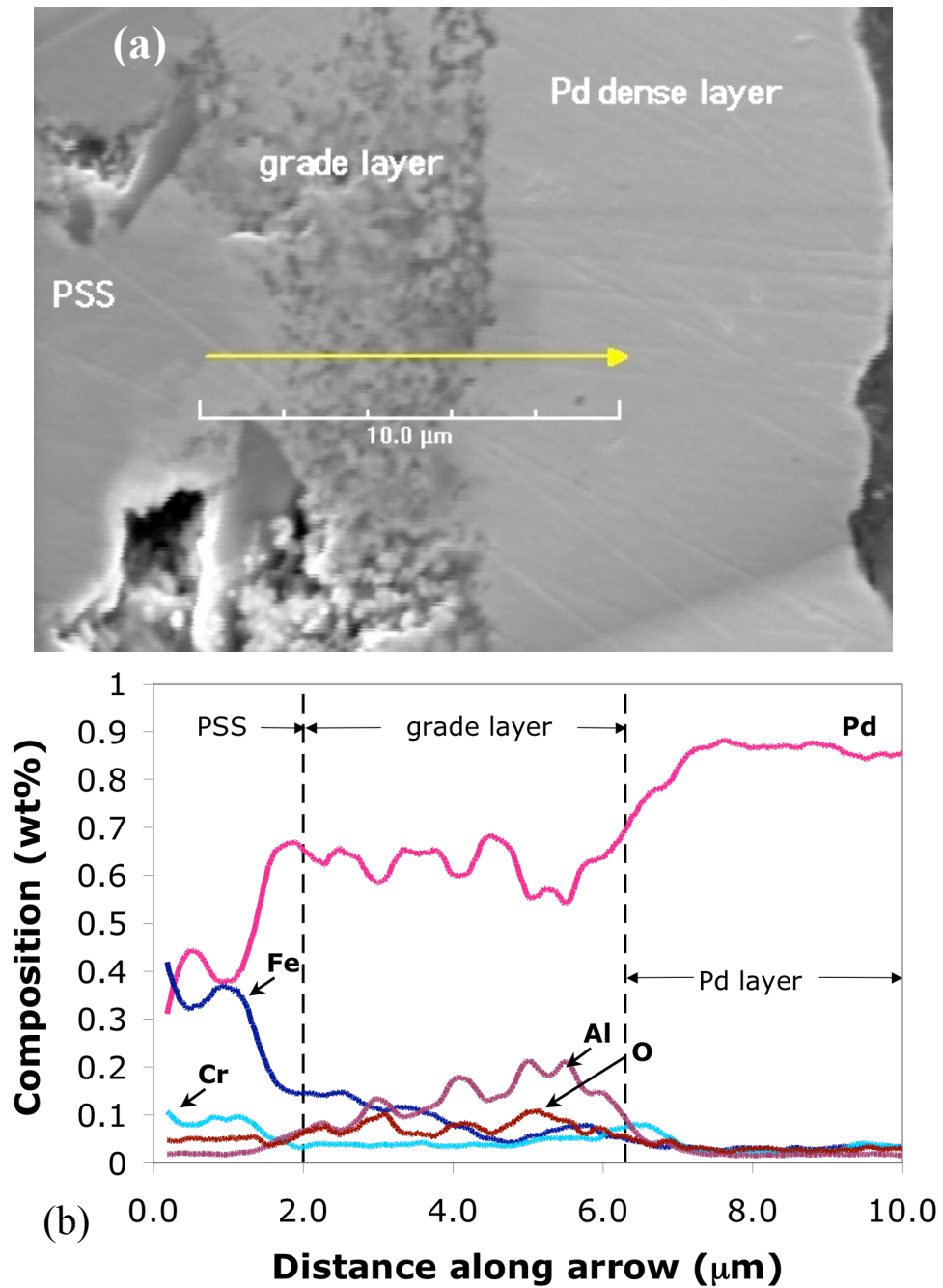


Figure 6-17 Composition analysis across the grade layer for the sample heated at  $600^\circ\text{C}$  in  $\text{H}_2$  (a) SEM micrograph (b) Elemental analysis along arrow.

## 6.4 Conclusions

This chapter detailed a new and unique procedure to achieve ultra-thin composite Pd membranes on porous metal supports, which were characterized by rough surfaces and broad pore size distribution at the surface. The deposition of pre-activated Al<sub>2</sub>O<sub>3</sub> particles followed by short time of Pd deposition led to a structure where big particles blocked pore mouths, fine particles filled the pores and very fine particles smoothed and narrowed the pore size distribution at the surface of the porous metal support. Pd layers deposited on such modified surfaces were very uniform and very thin. Thin membranes prepared on “graded” supports exhibit H<sub>2</sub> permeances as high as 21 m<sup>3</sup>/(m<sup>2</sup> h bar<sup>0.5</sup>) at 250°C and as high as 50 m<sup>3</sup>/(m<sup>2</sup> h bar<sup>0.5</sup>) at 500°C. However, the H<sub>2</sub> permeance of a freestanding Pd layer with the same thickness of 5.6 μm as that of Ma-42 was estimated to be 96 m<sup>3</sup>/(m<sup>2</sup> h bar<sup>0.5</sup>) at 500°C. Mass transfer resistance within the pores of the support was responsible for the lower H<sub>2</sub> permeance measured on the composite Ma-42 membrane. Composite Pd membranes were also characterized by good mechanical stability and very high selectivities (H<sub>2</sub>/He), which were higher than 1000 at temperatures equal to or lower than 400°C. The selectivity of all composite Pd membranes decreased at temperatures higher than 450°C. Finally, and most important, the H<sub>2</sub> permeance and the selectivity (H<sub>2</sub>/He) of this composite Pd membranes prepared on graded supports were stable over 1100 hr at 500°C, which represented a major breakthrough of the formation of thin composite Pd membranes.

---

## **7 Synthesis of composite Pd-Cu membranes on engineered substrate surface**

### **7.1 Introduction**

Pd-Cu membranes are believed to be more robust than pure Pd membranes since Pd-Cu alloys absorb less H<sub>2</sub>, thereby, being less prone to the problems related to the expansion upon H<sub>2</sub> absorption. In a previous preliminary work (Guazzone, 2003, PhD proposal), the synthesis of composite Pd-alloy membranes on 316L 0.5 μm grade PSS supports represented a challenge. Since Pd and Cu could not be co-deposited from electroless plating baths, the two metals had to be sequentially deposited and heat-treated to form the Pd-Cu alloy (“coating and diffusion” technique). While applying the “coating and diffusion” technique for the preparation of Pd-Cu alloys on 316L 0.5 μm grade PSS supports, several difficulties were encountered. The alloying of the Pd and Cu layers was limited by temperature since high temperatures ( $T > 550\text{-}600^\circ\text{C}$ ) led to intermetallic diffusion and the formation of large leaks. If low temperatures were used ( $500^\circ\text{C}$ ), thin Pd and Cu layers were preferred in order to decrease the annealing time, hence, a Pd-Cu-Pd-Cu – etc... structure was needed. However, plating Pd on top of Cu was not possible since the ammonia in the Pd plating bath dissolved part of the Cu layer. An attempt to plate Pd and Cu followed by heat-treatment and repetition of the Pd/Cu deposition and annealing steps several times was made to achieve a gas tight composite Pd-Cu membrane. Such tech-



nique was tedious and success was not guaranteed since some of the membranes came out black after any of the annealing steps. For the rare cases when the Pd-Cu had an acceptable appearance, large chemical gradients across the membrane layer were found.

The main difficulty in the synthesis of composite Pd-Cu membranes is the fact that no chemical gradients across the thickness of the alloy layer are allowed since Pd-Cu alloys only exhibit a sharp maximum in H<sub>2</sub> permeance at exactly Pd-Cu 40. Deviations from the optimal composition led to a drastic decrease in H<sub>2</sub> permeance (McKinley, 1967), which was due to the changes in relative amount of  $\alpha$  and  $\beta$  phase. For instance at 500°C<sup>1</sup>, the relative amount of  $\beta$  phase is 92% with 42 wt% Cu and only 54% with 40 wt% Cu. It became clear that to achieve a composite Pd-Cu 40wt% membrane, prepared with only one annealing step, the total thickness of the two metal layers, Pd and Cu, needed to be thin and not exceeding 5-10  $\mu\text{m}$ . The preparation of such a thin composite Pd membrane on a 0.5  $\mu\text{m}$  grade PSS supports was discarded due to the thick Pd layers (30-50 $\mu\text{m}$ ) needed to achieve a dense layer on 0.5  $\mu\text{m}$  grade PSS supports. A composite Pd-Cu 40wt% membrane could be achieved on a graded PH support yet the preparation of such a composite membrane was not undertaken. Morreale et al. (2004) recently proved that the low H<sub>2</sub> permeable Pd-Cu  $\alpha$  phase was more resistant to sulfur poisoning than the highly permeable  $\beta$  phase. Therefore, a low (10-20wt%) Cu content Pd-Cu alloy membrane would preferably be used at high temperatures (>500°C) in a H<sub>2</sub>S contaminated atmosphere.

The objective of the work described in this chapter was twofold. First, a fundamental study by means of High Temperature X-Ray Diffraction (HTXRD) on the nucleation of

---

<sup>1</sup> Relative amounts of  $\alpha$  and  $\beta$  phase can be calculated at any temperature using the lever rule on the portion of the Pd-Cu phase diagram shown in Figure 7-14, page 196.

---

the  $\beta$  phase in Pd-Cu alloys was carried out along with a study on the alloying mechanism of Pd-Cu bi-metallic layers. Secondly, from a more practical point of view, the work described in this chapter aimed at the possibility of preparing a thin ( $<10\mu\text{m}$ ) and stable low Cu content (10wt%Cu) Pd-Cu membrane on a graded PH support.

## 7.2 Theory

### 7.2.1 *The study of metal transformations with XRD*

The ordering  $\alpha(\text{fcc}) \rightarrow \beta(\text{bcc}) + \alpha(\text{fcc})$  transformation is shown in Figure 7-1 for an hypothetical Pd-Cu 39wt% cooled from  $620^\circ\text{C}$  to  $500^\circ\text{C}$ . If the alloy is kept at  $500^\circ\text{C}$  for a sufficiently long amount of time the equilibrium amount of  $\beta$  phase is given by the lever rule shown in Equation (7-1)

$$X_{\beta, \text{equilibrium}}(500^\circ\text{C}) = \frac{\overline{bc}}{\overline{ac}} \quad (7-1)$$

However, ordering transformations are nucleation and growth type of transformations. The growth of the  $\beta$  phase is shown with the dashed arrow starting at point c and ending at point b. Nucleation can also occur simultaneously with growth. At any time between point c and b the amount of  $\beta$  phase is given by the lever rule and denoted as  $X_\beta$ .

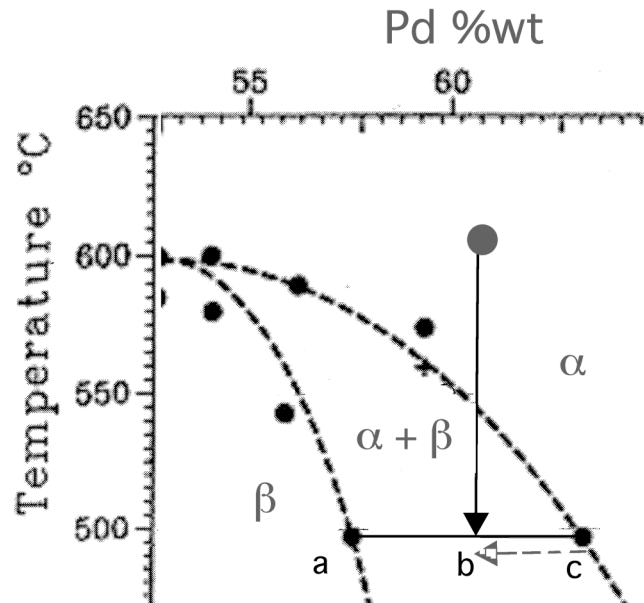


Figure 7-1  $fcc \rightarrow bcc$  ordering transformation in PdCu alloys

The rate at which the  $\alpha(fcc) \rightarrow \beta(bcc) + \alpha(fcc)$  transformation occurs depends on the thermodynamic driving force i.e.  $X_{\beta, equilibrium}$  and the diffusion rate of species, Pd and Cu atoms in this case. If the system temperature is dropped from 620°C to 550°C the thermodynamic driving force for the transformation is small yet the diffusion is high. If the system temperature is dropped from 620°C to 300°C the thermodynamic driving force is very high yet the diffusion is slow. These kinetic phenomena are characteristic of phase transformations in many metallic systems (Porter and Easterling, 1981). When cooling the hypothetical Pd-Cu 39wt% from 620°C to temperatures between 300 and 550°C a

maximum transformation rate should be found. The rate at which the transformation occurs,  $X_\beta$  vs. time, can be followed by XRD techniques in a HTXRD diffractometer by simultaneously collecting the (111) reflection of the  $\alpha$  phase and the (110) reflection of the  $\beta$  phase as a function time. The simultaneous collection of both reflections was possible with an LPD detector taking a  $2\theta$  range of  $10^\circ$ . The (111) reflection of the  $\alpha$  phase and the (110) reflection of the  $\beta$  phase were collected every 15 seconds.  $X_\beta$  was determined from XRD data using integrated intensities according to Equation (7-2)

$$X_\beta = \frac{I_\beta}{I_\beta + I_\alpha} \quad (7-2)$$

The rate of the transformation at a given temperature has to be normalized with the amount of  $\beta$  phase at equilibrium at the temperature T since  $X_{\beta, \text{equilibrium}}$  depends on the temperature the system is cooled to (see Figure 7-1). Hence, the rate of the ordering reaction is given by  $X_\beta / X_{\beta, \text{equilibrium}}$  as a function of time. The transformation at a given temperature,  $X_\beta$  vs. time, can then be plotted on the Pd-Cu phase diagram by placing  $X_\beta(t)$  between the  $\beta/(\alpha+\beta)$  and  $(\alpha+\beta)/\alpha$  boundaries according to the lever rule, Equation (7-1).

## 7.3 Experimental

### 7.3.1 XRD sample preparation

The bimetallic Cu-Pd- $\text{Al}_2\text{O}_3$  samples consisted of a thin Pd layer covered by a thin Cu layer on a sintered  $\alpha\text{-Al}_2\text{O}_3$  substrate ( $1 \times 1.5$  cm, thickness 2 mm). Prior to Pd and Cu deposition, the  $\alpha\text{-Al}_2\text{O}_3$  substrates were treated at  $800^\circ\text{C}$  in air for 12 hr for cleaning purposes and seeded with Pd nuclei by alternatively immersing the substrates in  $\text{SnCl}_2$  (1 g/l,

---

pH=2) and PdCl<sub>2</sub> (0.1 g/l, pH=2) solutions. Pd and Cu were deposited by the electroless plating method using the plating bath composition listed in Table 7-1. The thickness and Cu content of each layer was determined by the gravimetric method. Since the  $\alpha$ -Al<sub>2</sub>O<sub>3</sub> substrates were totally immersed in the plating bath, each sample had two faces. The studied face was numbered as “face 1” and the opposite face laying on top of the Pt-Rh heating strip was numbered as “face 2”. Three different Cu-Pd- $\alpha$  Al<sub>2</sub>O<sub>3</sub> samples were considered: Pd/Cu-40wt% (sample Pd-Cu-1), Pd/Cu-46wt% (sample Pd-Cu-2) and Pd/Cu-50wt% (sample Pd-Cu-3). Table 7-2 lists all samples analyzed in this study. Cu-Pd- $\alpha$  Al<sub>2</sub>O<sub>3</sub> samples were initially heat-treated by raising the temperature from room temperature to 650°C in less than 2 minutes. A dwell time ranging from 4 to 6 hr was set so that the chemical composition across the thicknesses of the layer was homogeneous. After homogenization, the samples were cooled in three different ways: a fast quench to room temperature (sample Pd-Cu-1), a slow ramp (3°C/min) to room temperature (sample Pd-Cu-2) and, for sample Pd-Cu-3, a quench to 400°C (dwell time 2 min) followed by a dwell at 525°C (2 hr) and a slow cool down to room temperature. All temperature changes and annealing steps were carried out in He atmosphere.

*Table 7-1 Chemical composition of Pd and Cu plating bath*

Chemical	Pd Bath	Cu Bath	Function
Pd(NH <sub>3</sub> ) <sub>4</sub> Cl <sub>2</sub> ·H <sub>2</sub> O (g/l)	4	-	Pd <sup>2+</sup> ions source
CuSO <sub>4</sub> ·5H <sub>2</sub> O (g/l)	-	20	Cu <sup>2+</sup> ions source
Na <sub>2</sub> EDTA 2H <sub>2</sub> O (g/l)	40.1	30	Complexant-stabilizer
NH <sub>4</sub> OH (28%) (ml/l)	198	-	Buffer
H <sub>2</sub> NNH <sub>2</sub> (1 M) (ml/l)	5.6	-	Reducing agent
HCHO (37%) (ml/l)	-	14	Reducing agent
EDA (ppm)	-	100	Grain refiner
K <sub>4</sub> Fe(CN) <sub>6</sub> ·3H <sub>2</sub> O (ppm)	-	35	Accelerator
(C <sub>2</sub> H <sub>5</sub> ) <sub>2</sub> NCS <sub>2</sub> Na·3H <sub>2</sub> O (ppm)	-	5	Stabilizer
pH	10-11	12-13	
Temperature (°C)	60	20-25	

The alloying process of the Cu-Pd-substrate composite structures, as well as the ordering fcc → bcc transformation taking place in Pd-Cu alloys, were studied using the time resolved HTXRD described in Section 3.4.2.1.

*Table 7-2 List of Pd-Cu samples used in this Chapter*

Sample	support	Cu content (wt% from gravimetric)	Experiment
Pd-Cu-1	α-Al <sub>2</sub> O <sub>3</sub>	40	Annealed, quenched (650°C to 20°C)
Pd-Cu-2	α-Al <sub>2</sub> O <sub>3</sub>	46	Annealed, slowly cooled (650 to 20°C at 3°C/min)
Pd-Cu-3	α-Al <sub>2</sub> O <sub>3</sub>	50	Annealed, quenched to 400°C (dwell, 2min), heated at 525°C for 2 hr, slowly cooled 20°C
Pd-Cu-4a	PH	41	β phase nucleation rate (1 <sup>st</sup> experiment)
Pd-Cu-4b	PH	41	β phase nucleation rate (2 <sup>nd</sup> experiment)

### 7.3.2 The preparation of a composite Pd-Cu membrane, Ma-41

The composite Pd-Cu membrane, Ma-41, was prepared by the coating and diffusion technique. The coarse PH support was characterized, cleaned, graded and activated according to Sections 3.1.1-3.1.3. A 5μm thick Pd layer and a 2μm thick Cu layer were sequentially deposited by the electroless plating method using the metal plating baths

listed in Table 7-1. The composite Cu-Pd-PH structure was annealed in H<sub>2</sub> atmosphere by holding the membrane for 12-24 hr at each of the following temperatures: 250, 300, 350, 400, 450, 500 and 550°C. After the annealing process, the surface of the membrane had a silver color with a slight orange tint. Finally, the annealed Pd-Cu membrane was coated with an additional 3μm of Pd to achieve a leak free membrane. Figure 7-2 and Figure 7-3 show the silver color of Ma-41's surface and the entire support respectively.

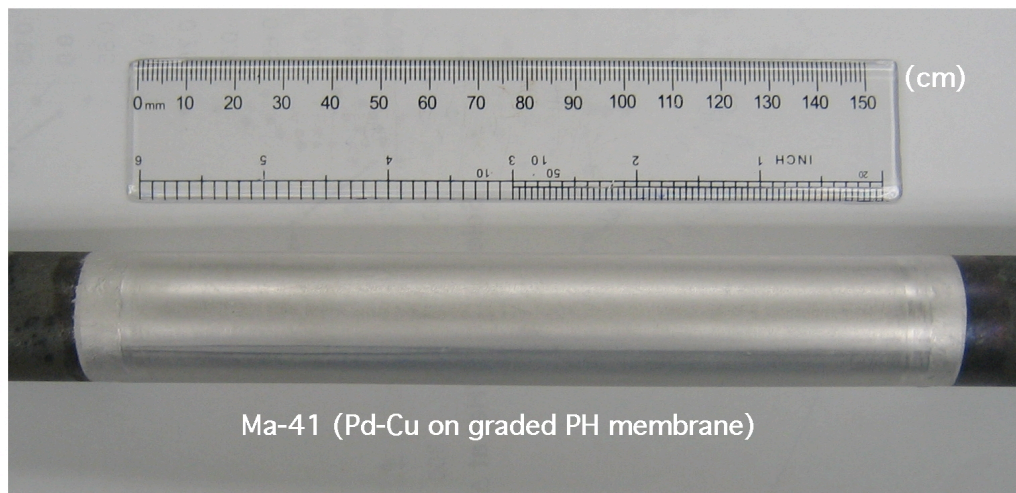


*Figure 7-2 Ma-41 composite Pd-Cu membrane*

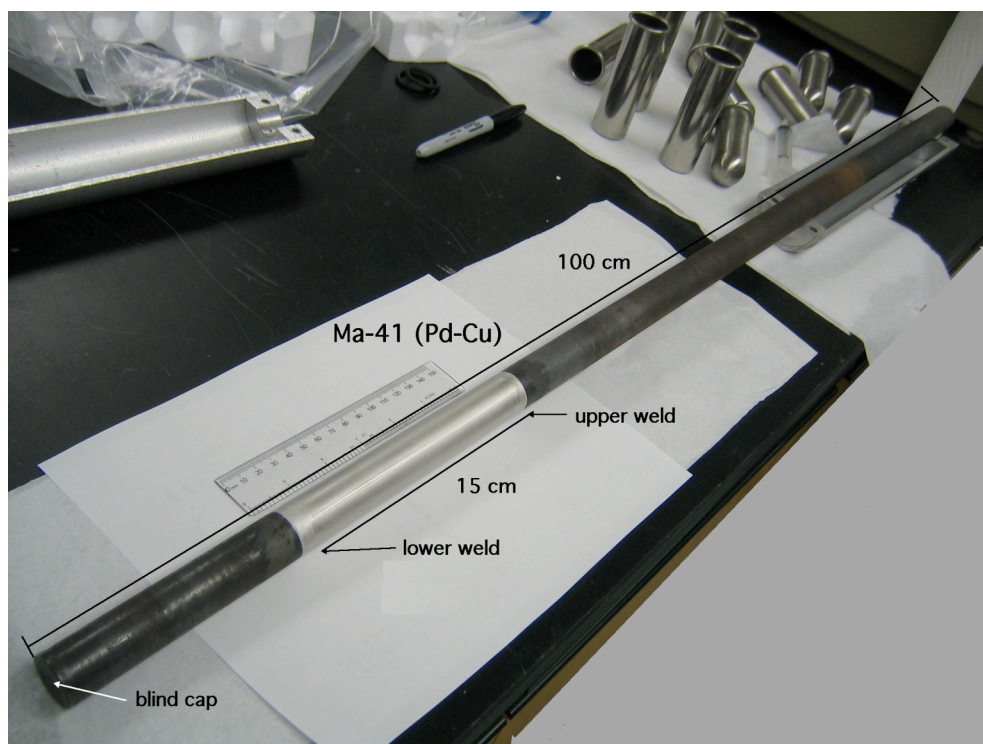


*Figure 7-3 Ma-41 composite Pd-Cu membrane*



---

The total surface of the H<sub>2</sub> permeable membrane was 120 cm<sup>2</sup> and its thickness was estimated to be 10 μm. The membrane was characterized in H<sub>2</sub> atmosphere as described in Section 3.2. The He leak of the membrane was measured either in pure He atmosphere or in H<sub>2</sub> atmosphere by feeding the shell side with a 99%H<sub>2</sub>-1%He mixture gas and analyzing the tube flow with Gas Chromatography (GC). UHP H<sub>2</sub> was used as the carrier gas and the TCD detector gain was set to high.

## 7.4 Results and discussion

### 7.4.1 *The inter-diffusion of Pd-Cu bi-layers*

Figure 7-4 shows the phase transformation in sample Pd-Cu-1 taking place at 650°C as a function of time. The first two patterns only showed the two distinctive fcc phases of Pd and Cu. The intensity of the Pd (111) and Cu (111) reflections rapidly decreased and within 6 min (3<sup>rd</sup> pattern) the peaks of pure Pd and Cu phases were no longer visible. Instead, a Cu rich fcc phase with very broad peaks, due to large concentration gradients, were seen in the 3<sup>rd</sup> pattern. As Cu atoms diffused into the Pd layer, the Cu rich fcc phase faded out and the peaks of a Pd rich fcc phase appeared in the 4<sup>th</sup> pattern. In addition, since concentration gradients disappeared, peaks became sharper (pattern 4 to 20). After 40 minutes at 650°C no further changes took place in the XRD patterns, which theoretically corresponded to a homogeneous Pd-Cu alloy. The sample was held at 650°C for a total time of 5 hr.

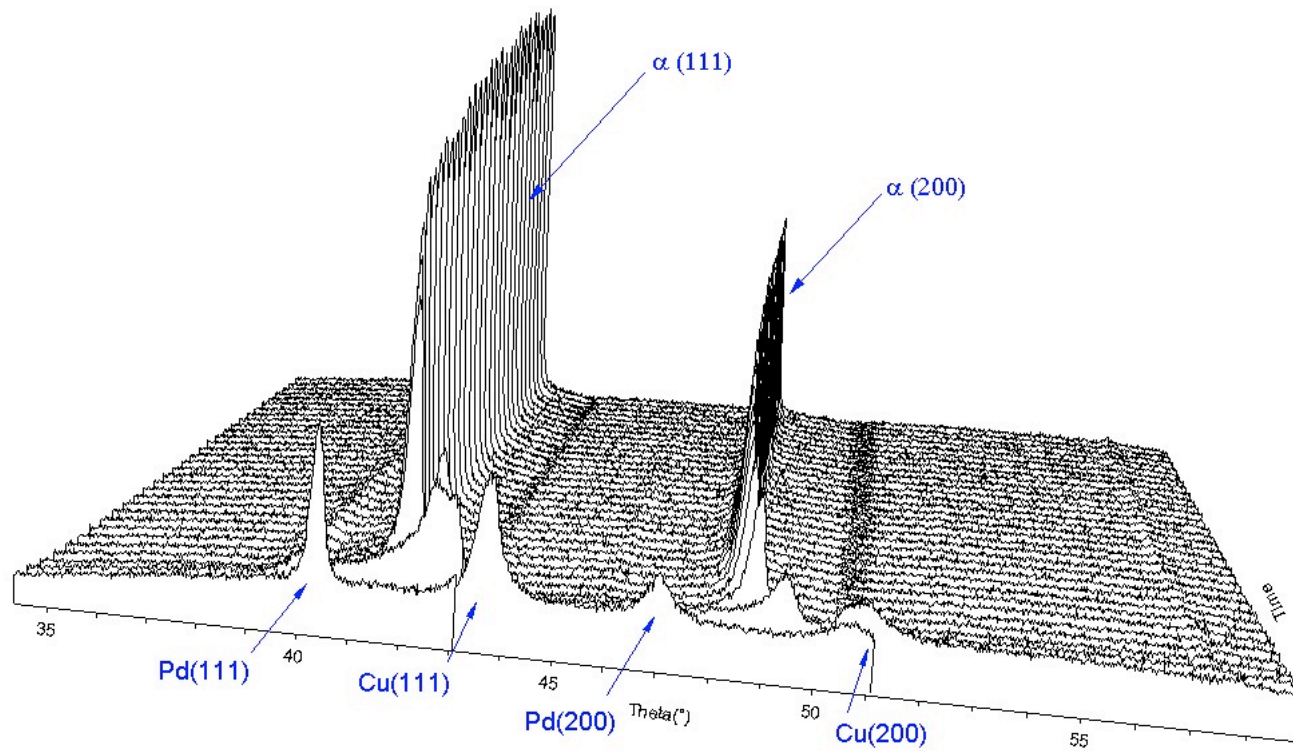


Figure 7-4 Phase changes as a function of time in sample n1 (650°C in He)

However, the existence of very small concentration gradients were not excluded. Therefore, in order to ensure homogeneity the temperature was increased up to 800°C for 30 minutes. Sample Pd-Cu-1 was then quenched to room temperature. No ordered bcc  $\beta$  phase nucleated indicating that either the  $\alpha$  phase stable at 800°C was retained after the fast drop in temperature, or the Cu concentration of sample Pd-Cu-1 fell outside the coexistence domain of the  $\beta$  and  $\alpha$  phase (i.e. the Cu concentration was lower than ca. 30wt%). In the case the  $\alpha$  phase was retained, sample Pd-Cu-1 was heat-treated at 400°C in He in order to trigger the nucleation of the  $\beta$  phase. No nucleation took place indicating that the Cu concentration was lower than 30wt%. EDX analysis of sample Pd-Cu-1 surface indicated the presence of a Pd-Cu alloy with a Cu concentration of 27 wt% in agreement with the final fcc phase.

Figure 7-5(a) shows the phase transformation that occurred as a function of time at 650°C for sample Pd-Cu-2. The first two XRD patterns showed pure Pd and pure Cu peaks with decreasing intensities as diffusion took place (1<sup>st</sup> and 2<sup>nd</sup> pattern). However, in this case, two  $\alpha$  phases appeared in the 3<sup>rd</sup> pattern. The first  $\alpha$  phase, Pd rich, with (111) reflection exiting at  $2\theta$  ca. 41.1° was initially characterized by broad peaks due to concentration gradients. As diffusion occurred, the peaks of the Pd rich phase shifted from values of  $2\theta$  ca 41.1° to values of  $2\theta$  ca 40.5°, an indication of the progressive enrichment in Pd. Moreover, the peaks of the (111) reflection sharpened and increased in intensity indicating the growing of the Pd rich phase. The second  $\alpha$  phase, which was very rich in Cu, had a very sharp (111) reflection peak located at  $2\theta$  ca. 42°.

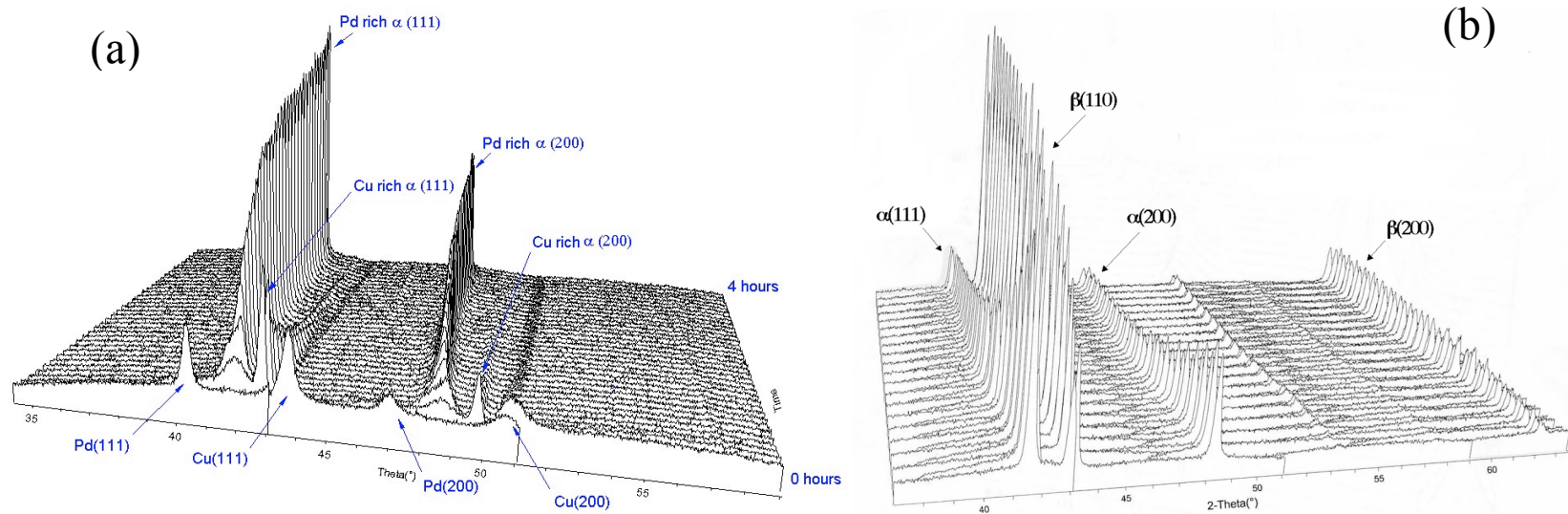


Figure 7-5 (a) left. XRD pattern collection of sample Pd-Cu-2 as a function of time. (650°C in He). (b) right. XRD pattern collection while cooling from 650°C to 300°C. Nucleation of the  $\beta$  phase occurred at a temperature above 525°C.